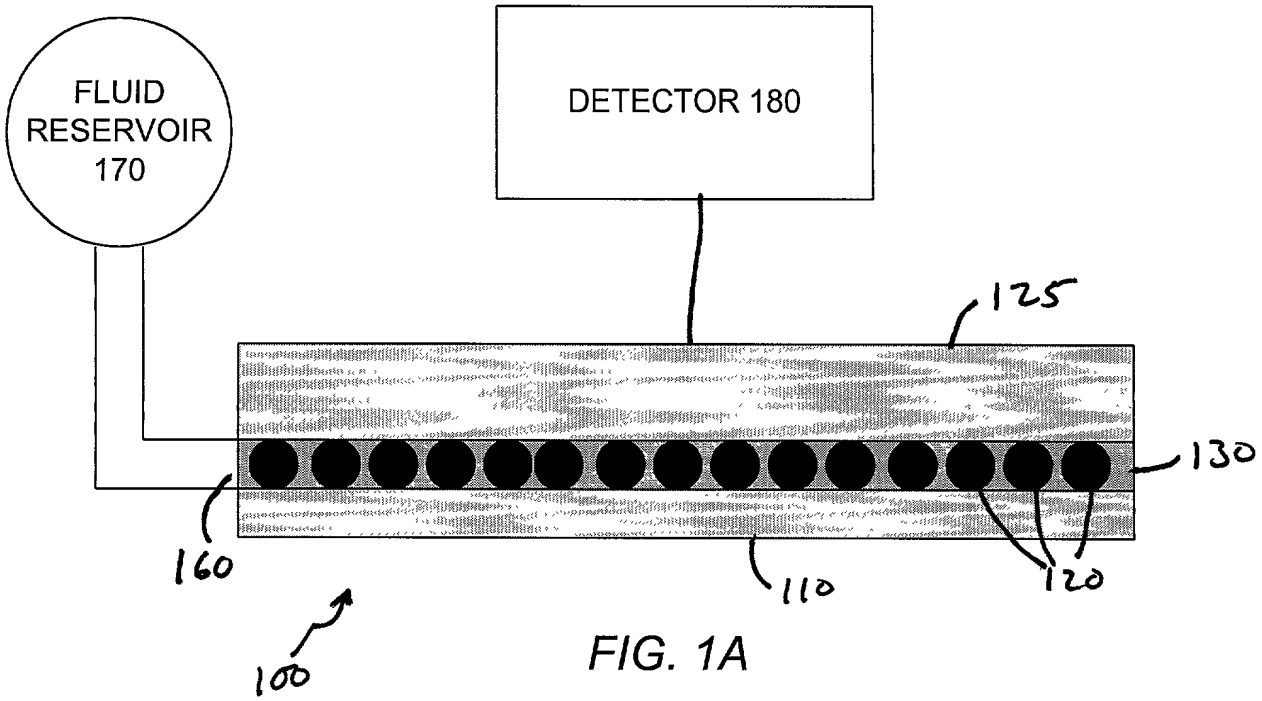

FIG. 1A

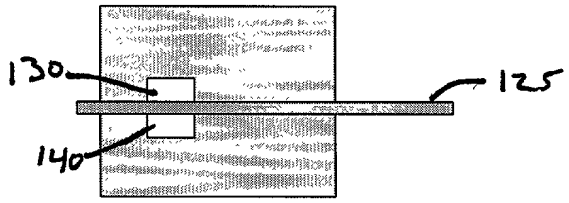

FIG. 1B

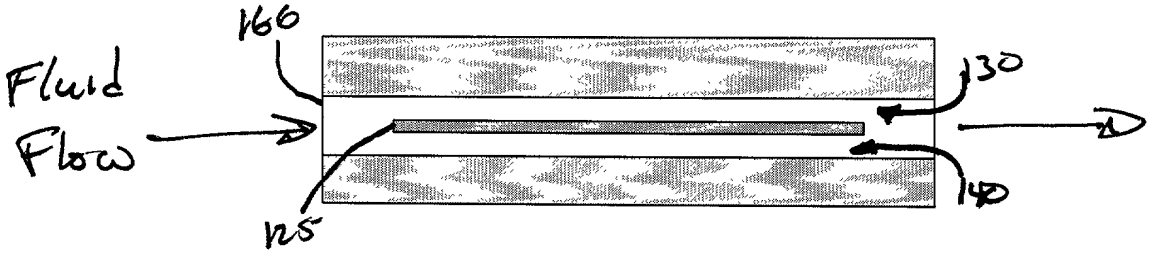

FIG. 1C

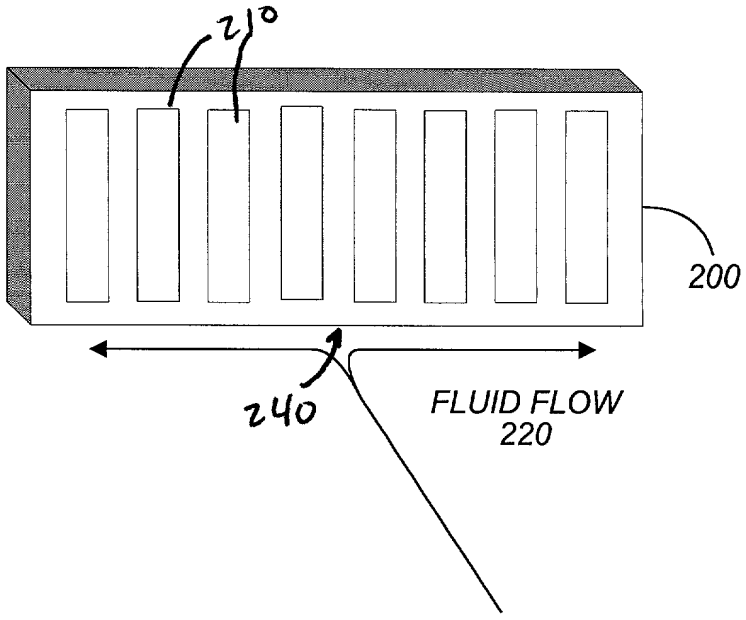

FIG. 2

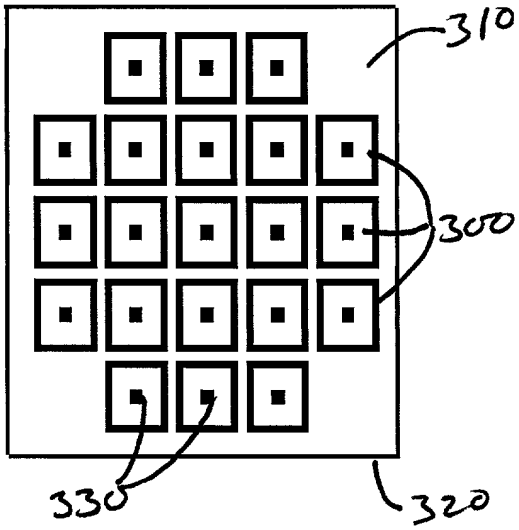

FIG. 3

Analyte Flow: Normal vs. Composite Sensors

Normal sensor- analyte flows across membranes

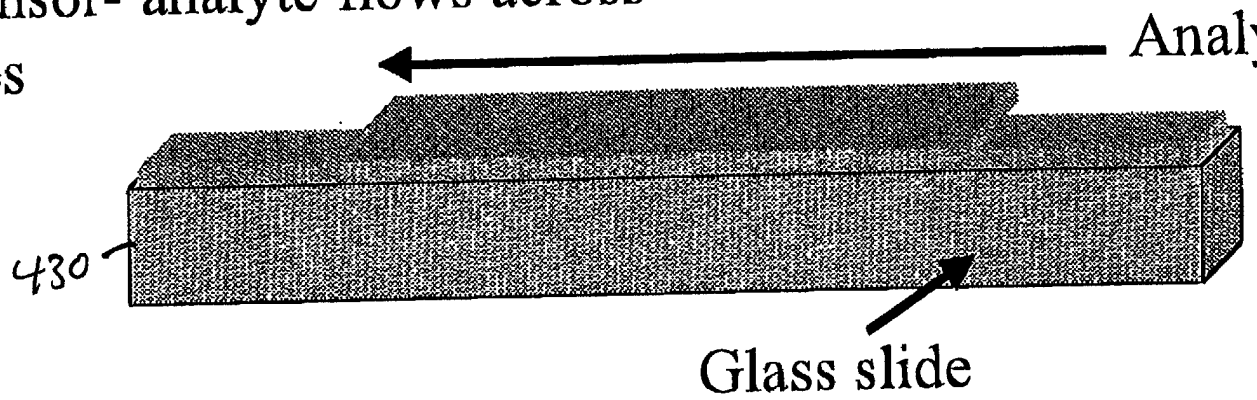

Composite sensor- analyte flows across and through membranes

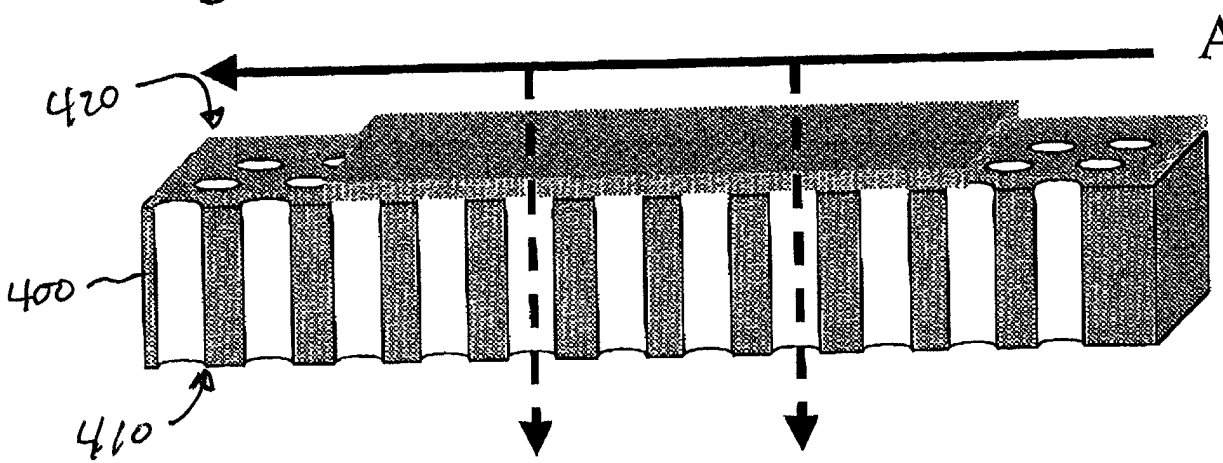

FIG. 4A

Schematic of Apparatus

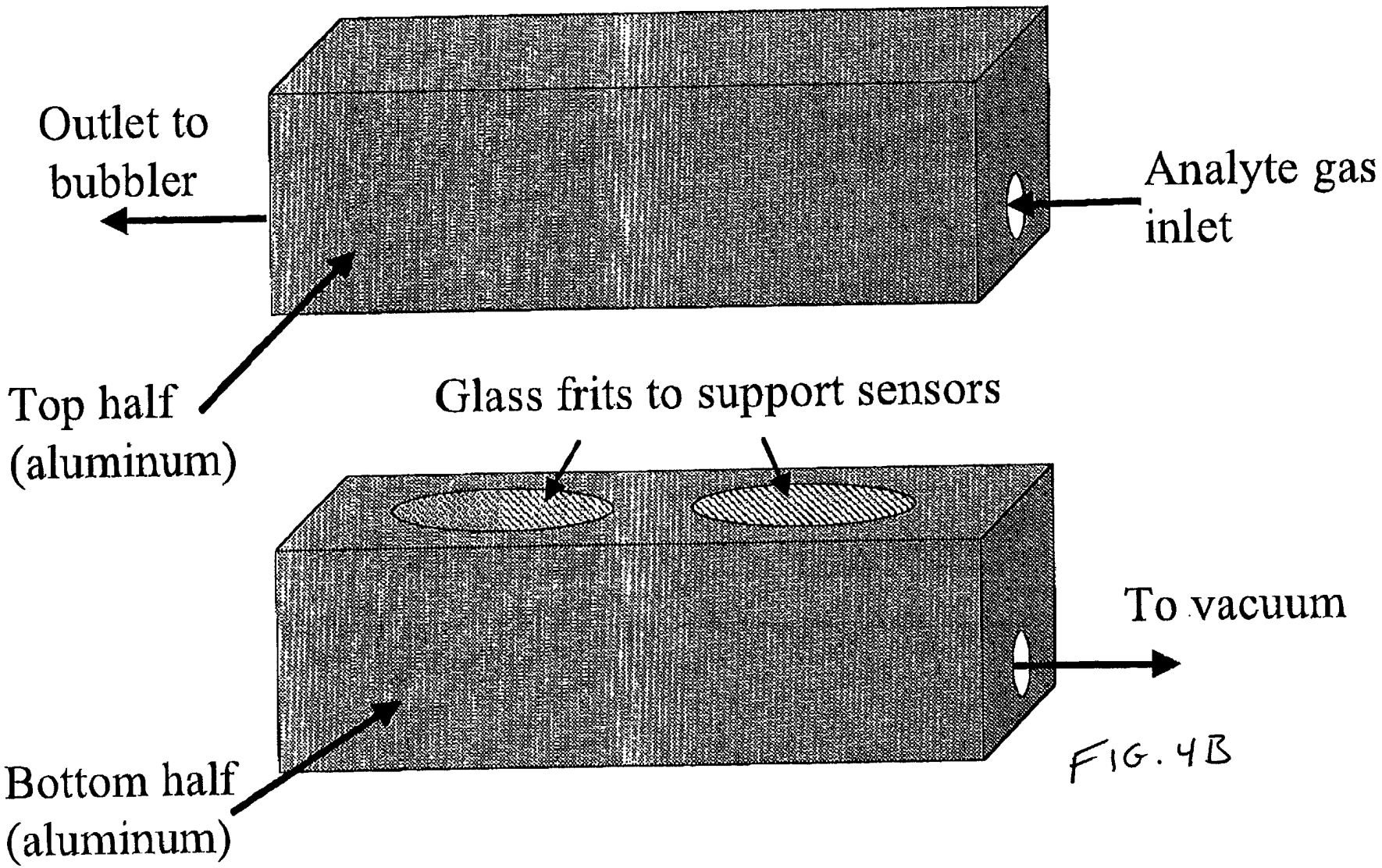

FIG. 4B

a) **face-view of substrate**

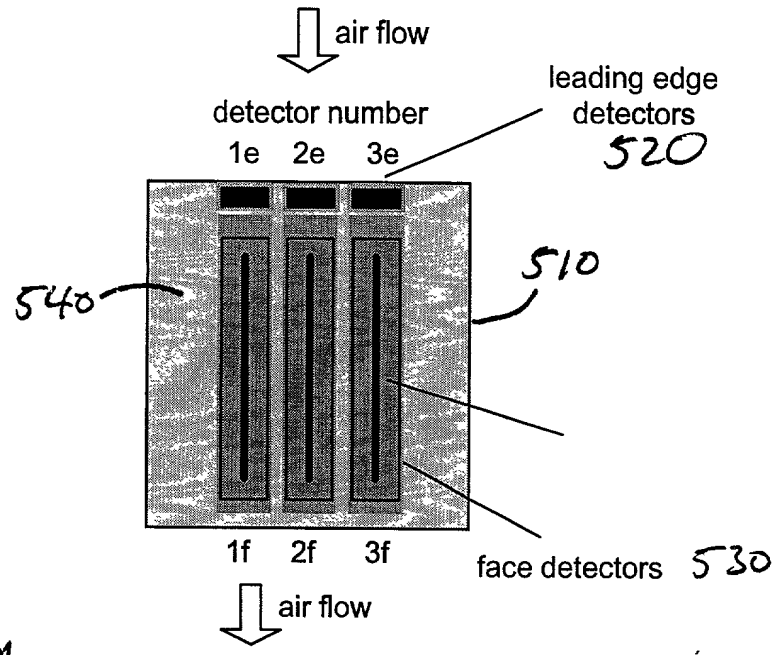

FIG. 5A

b) **leading edge-view of 2 substrates**

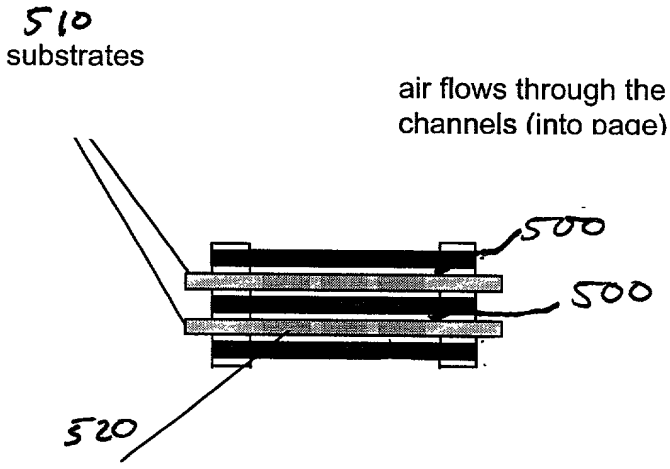

FIG. 5B

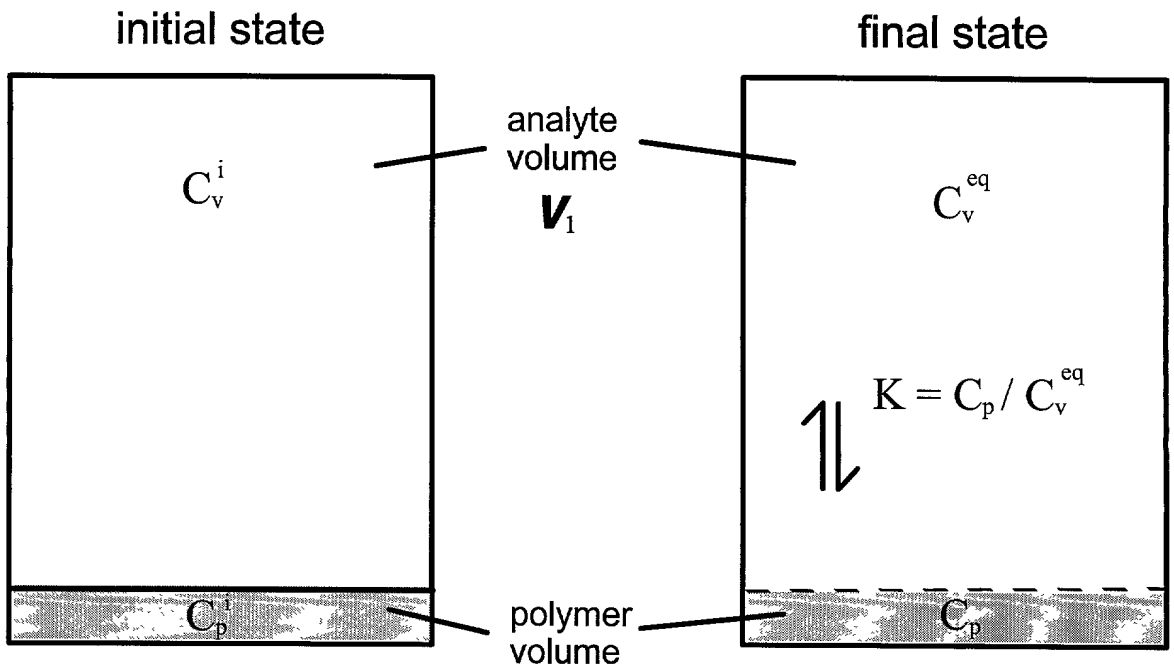

$$\Delta V_1 = -\Delta V_p \sim 0$$

FIG. 6

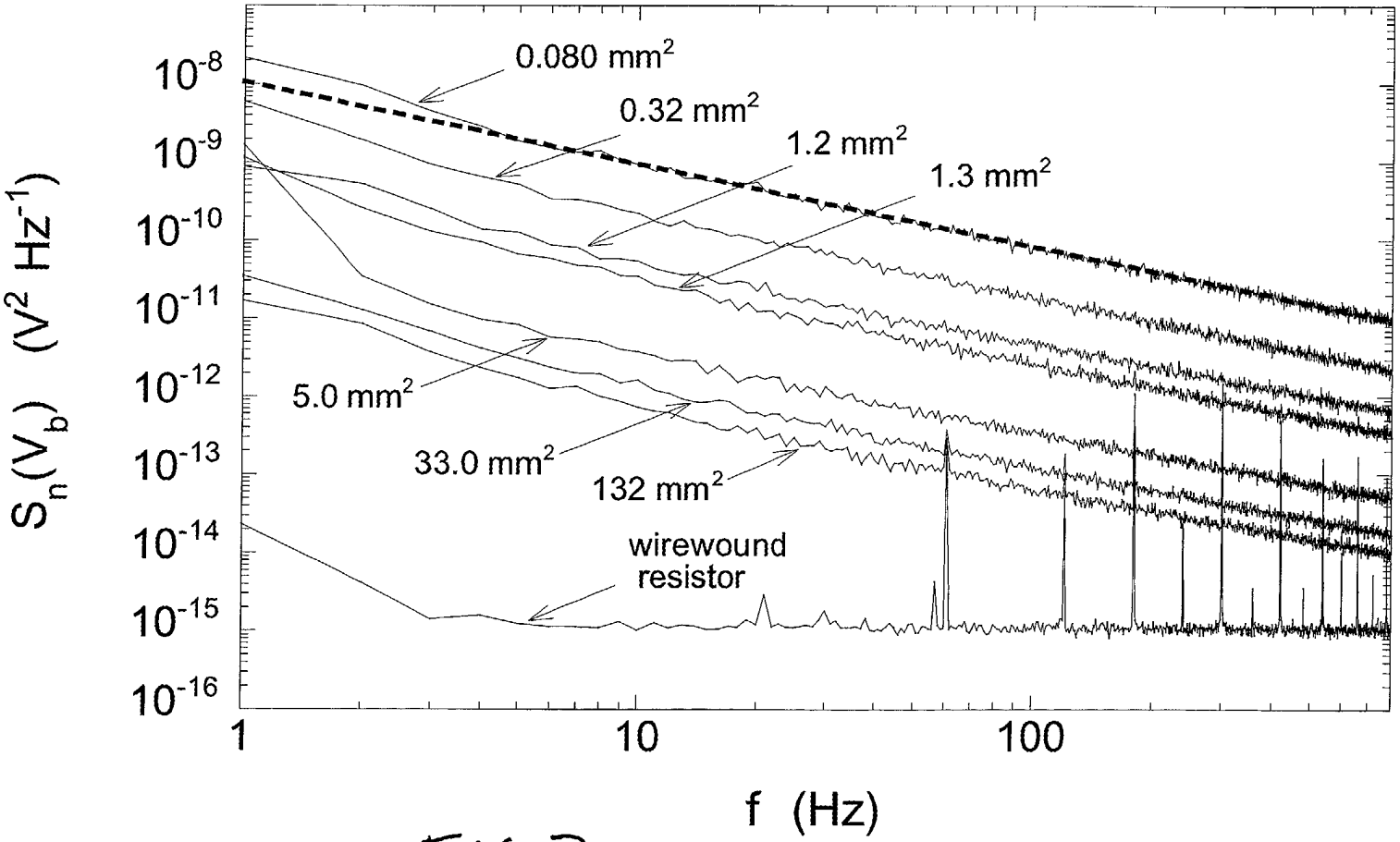

FIG. 7

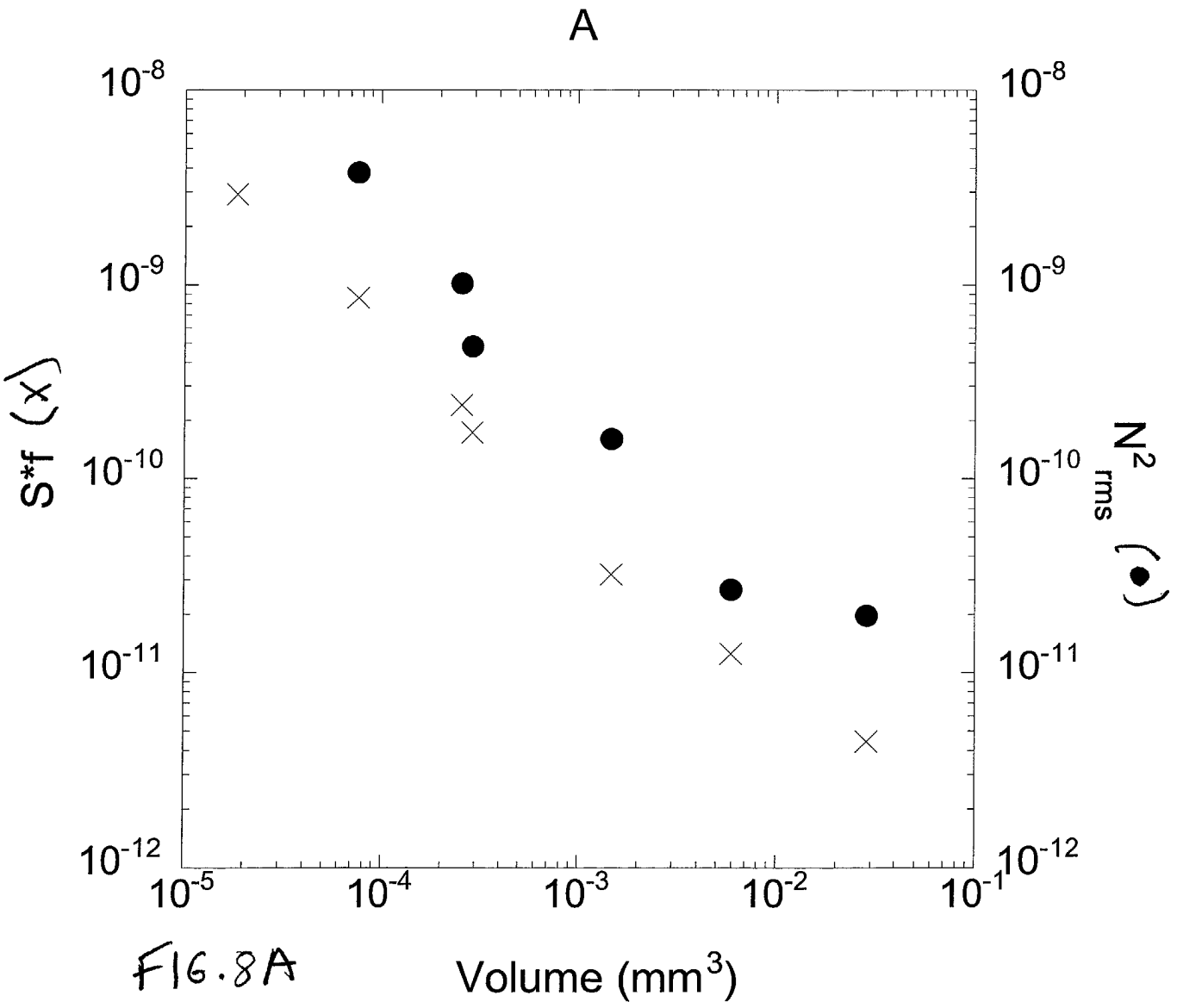

FIG. 8A

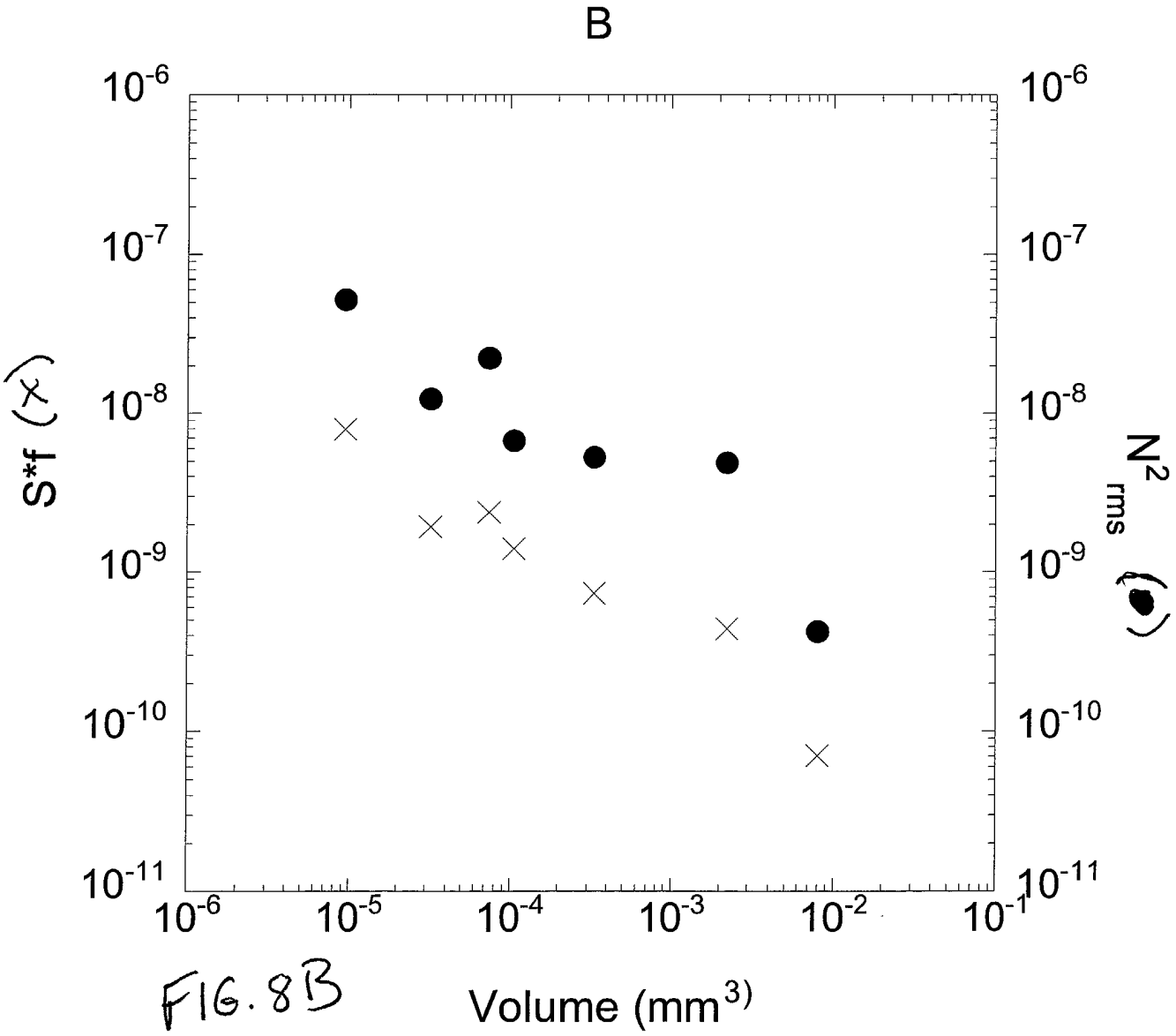

FIG. 8B

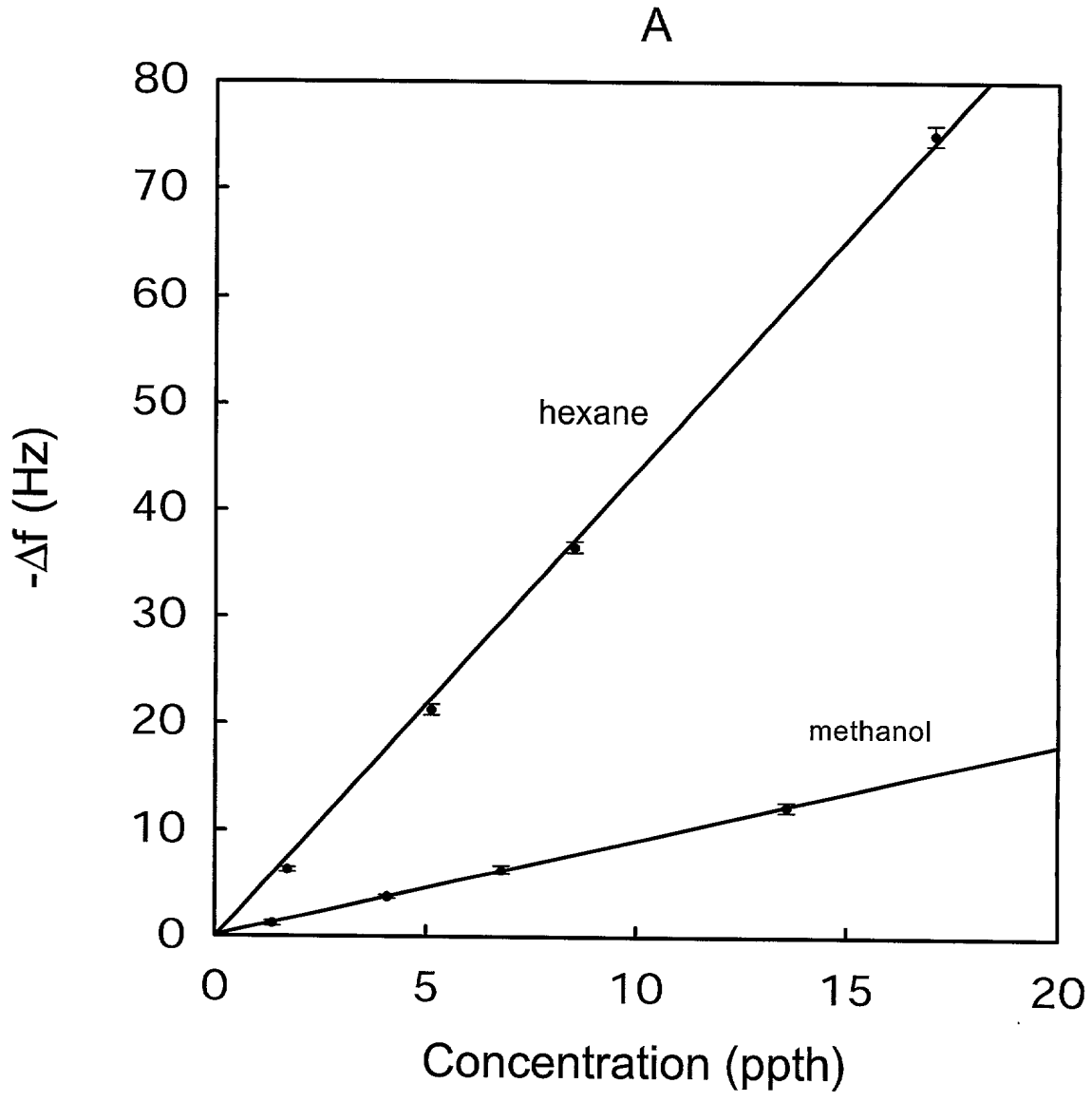
A
80
70
60
50
40
30
20
10
0
-Δf (Hz)
hexane
methanol
0
5
10
15
20
Concentration (ppth)

FIG. 9A

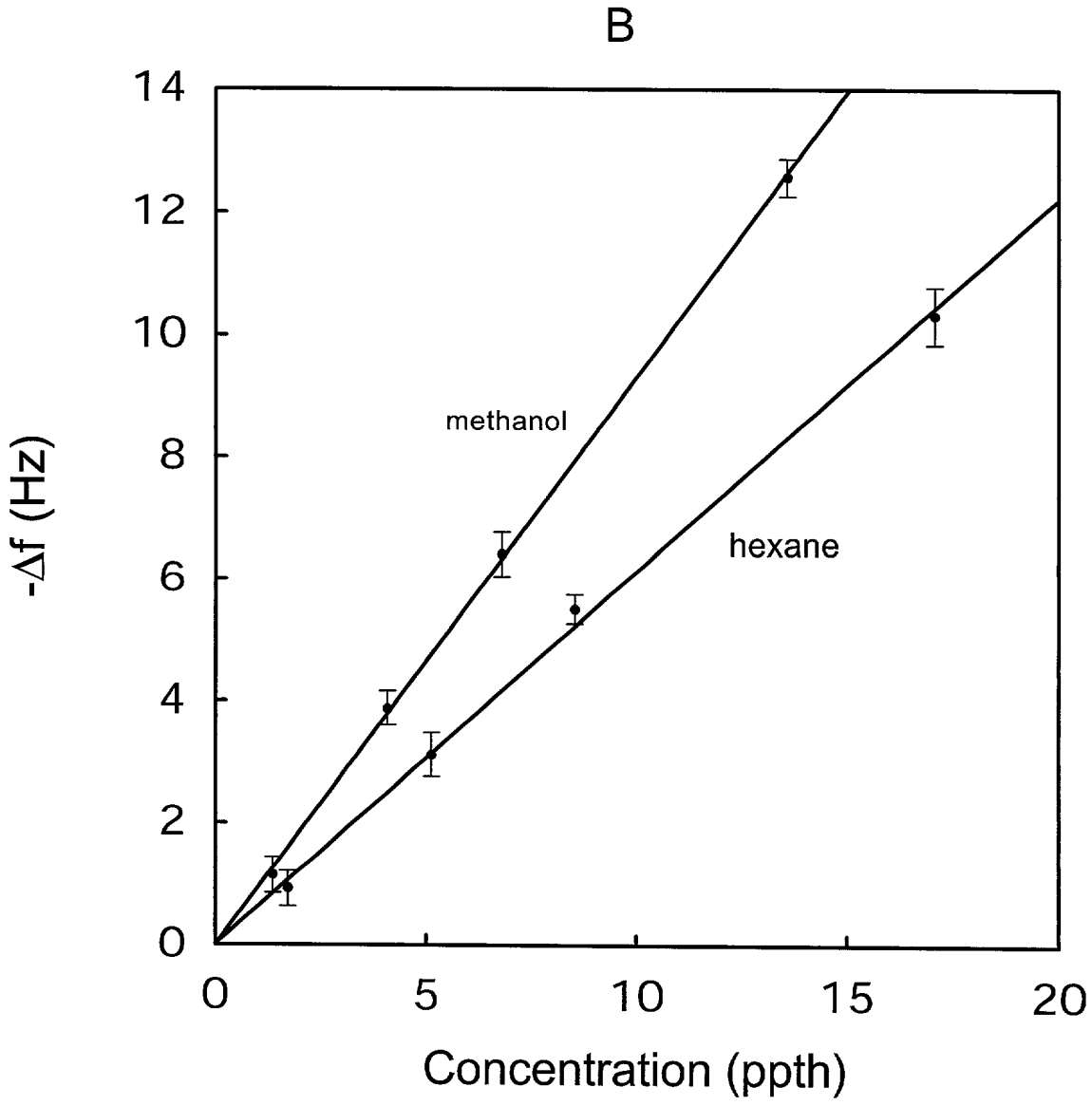
B
14
12
10
8
6
4
2
0
-Δf (Hz)
methanol
hexane
0
5
10
15
20
Concentration (ppth)

FIG. 9B

Responses, Noise, and S/N for two Types of Polymer-Carbon Black Composite Detectors in the Configuration of FIGS. 5A and 5B.[a]

Analyte	Vapor Pressure of Pure Analyte		log Partition Coefficient (log k)[b]		Stack Assembly	$\Delta R/R_b \times 100$				N_{rms}				S/N			
			PCL	PEVA		PCL		PEVA		PCL		PEVA		PCL		PEVA	
	P^o (Torr)	PPM[c]				edge[d]	face	edge	face	edge	face	edge	face	edge	face	edge	face
hexane	$1.28*10^{2}$	$1.71*10^{5}$	1.65	2.23	A	1.4±0.2	1.07±0.03	3.3±0.1	3.5±0.6	$(1.5±0.7)*10^{-3}$	$(1.9±0.5)*10^{-4}$	$(5±1)*10^{-4}$	$(8±2)*10^{-5}$	13±7	60±14	73±20	460±200
					B	1.1±0.4	0.77±0.04	3.6±0.3	2.5±0.1	$(2±1)*10^{-3}$	$(3.2±0.8)*10^{-4}$	$(9±2)*10^{-4}$	$(1.3±0.3)*10^{-4}$	5±2	26±9	44±12	200±45
					C	1.3±0.2	1.17±0.08	2.8±0.3	2.4±0.1	$(1.2±0.6)*10^{-3}$	$(1.8±0.2)*10^{-4}$	$(4±2)*10^{-4}$	$(2.7±0.9)*10^{-4}$	23±23	100±60	77±25	100±37
					mean	1.3	1.0	3.2	2.8	$2*10^{-3}$	$2.3*10^{-4}$	$6*10^{-4}$	$1.6*10^{-4}$	14	64	65	260
methanol	$1.02*10^{2}$	$1.36*10^{5}$	2.26	1.98	A	2.4±0.2	2.7±0.1	2.0±0.4	2.1±0.5	$(1.4±0.8)*10^{-3}$	$(2.0±0.5)*10^{-4}$	$(5±1)*10^{-4}$	$(9±2)*10^{-5}$	23±12	140±42	42±10	270±120
					B	3.3±0.5	2.4±0.2	1.8±0.3	1.61±0.08	$(3±1)*10^{-3}$	$(3.0±0.6)*10^{-4}$	$(9±2)*10^{-4}$	$(1.5±0.3)*10^{-4}$	14±5	80±16	21±5	120±25
					C	2.6±0.8	2.8±0.2	1.1±0.2	1.2±0.1	$(1.2±0.8)*10^{-3}$	$(1.3±0.7)*10^{-4}$	$(4±2)*10^{-4}$	$(2.6±0.9)*10^{-4}$	33±22	260±110	28±11	50±17
					mean	2.8	2.6	1.6	1.6	$2*10^{-3}$	$2.1*10^{-4}$	$6*10^{-4}$	$1.6*10^{-4}$	23	160	30	140
dodecane	$9.71*10^{-2}$	$1.29*10^{2}$	4.77[e]	5.35[e]	A	1.6±0.2	1.16±0.03	3.7±0.1	3.6±0.6	$(1.3±0.6)*10^{-3}$	$(2.0±0.4)*10^{-4}$	$(5±1)*10^{-4}$	$(9±0.3)*10^{-5}$	15±7	60±13	76±21	440±170
					B	1.2±0.4	0.88±0.07	3.8±0.3	2.6±0.1	$(3±1)*10^{-3}$	$(3.2±0.9)*10^{-4}$	$(9±2)*10^{-4}$	$(1.4±0.2)*10^{-4}$	5±2	30±10	45±14	190±35
					C	1.6±0.2	1.25±0.04	3.4±0.1	1.3±0.2	$(1.2±0.8)*10^{-3}$	$(9±5)*10^{-5}$	$(4±2)*10^{-4}$	$(2.5±0.7)*10^{-4}$	32±32	150±64	100±41	54±21
					mean	1.5	1.1	3.6	2.5	$2*10^{-3}$	$2.1*10^{-4}$	$6*10^{-4}$	$1.6*10^{-4}$	17	81	73	230
hexadecan	$9.11*10^{-4}$	1.21	6.70[e]	7.35[e]	A	0.3±0.2	0.01±0.09	0.26±0.09	0.01±0.01	$(1.4±0.9)*10^{-3}$	$(1.9±0.3)*10^{-4}$	$(5±1)*10^{-4}$	$(8±3)*10^{-5}$	3±2	1±1	6±2	2±2
					B	0.3±0.3	0.02±0.03	0.4±0.1	0.02±0.04	$(2±2)*10^{-3}$	$(3.1±0.9)*10^{-4}$	$(9±2)*10^{-4}$	$(1.4±0.3)*10^{-4}$	2±1	1±1	5±2	1±3
					C	0.3±0.2	0.03±0.03	0.3±0.1	0.04±0.07	$(1.1±0.7)*10^{-3}$	$(1.2±0.6)*10^{-4}$	$(4±2)*10^{-4}$	$(2.3±0.7)*10^{-4}$	5±4	4±4	8±3	2±3
					mean	0.3	0.02	0.3	0.03	$2*10^{-3}$	$2.1*10^{-4}$	$6*10^{-4}$	$1.5*10^{-4}$	3	2	6	2

a) Data were averages of 10 randomized presentations of the 4 analytes each at P/P^o =0.050, across 3 copies of each of the 2 detector types, with each value representing 30 vapor/polymer interactions. The experiment was repeated for 3 independently prepared stack assemblies (A,B,&C). The data represent responses after 200 s of exposure to analyte. b) Determined from quartz crystal microbalance measurements on unfilled polymers. c) Vapor pressure of analyte expressed in ppm of air at 294 K. d) Edge refers to the leading edge sensors and face refers to the face sensors depicted in FIGS. 5A and 5B. The uncertainties are expressed as 95% confidence intervals. e) Values were estimated based on measurements of K for hexane and correction for the differences in vapor pressure between hexane and the alkane of interest assuming constant activity coefficients for the sorption of the alkanes into a given polymeric phase.

FIG. 10

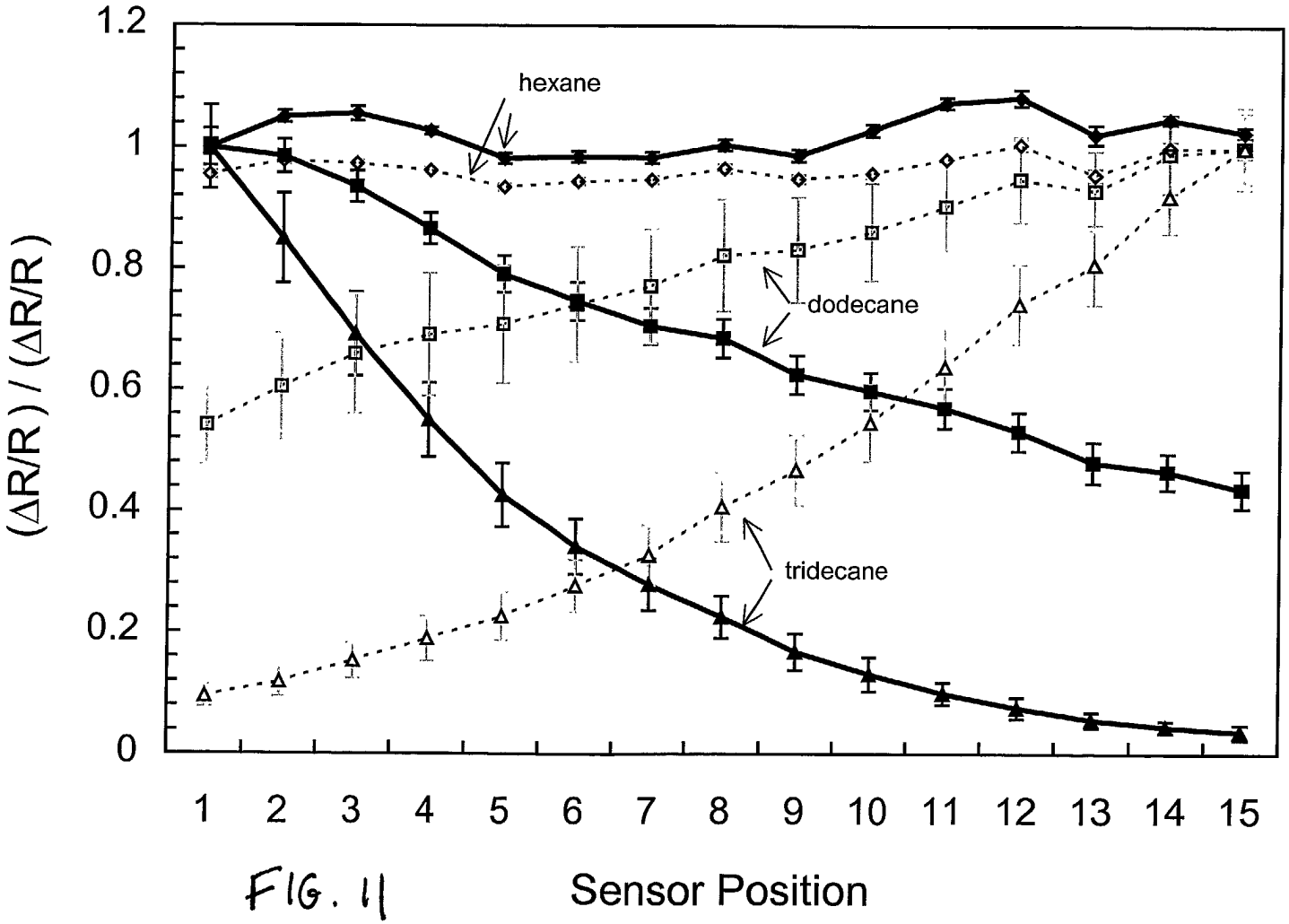
1.2
1
0.8
0.6
0.4
0.2
0
(ΔR/R) / (ΔR/R)
hexane
dodecane
tridecane
1
2
3
4
5
6
7
8
9
10
11
12
13
14
15
Sensor Position

FIG. 11

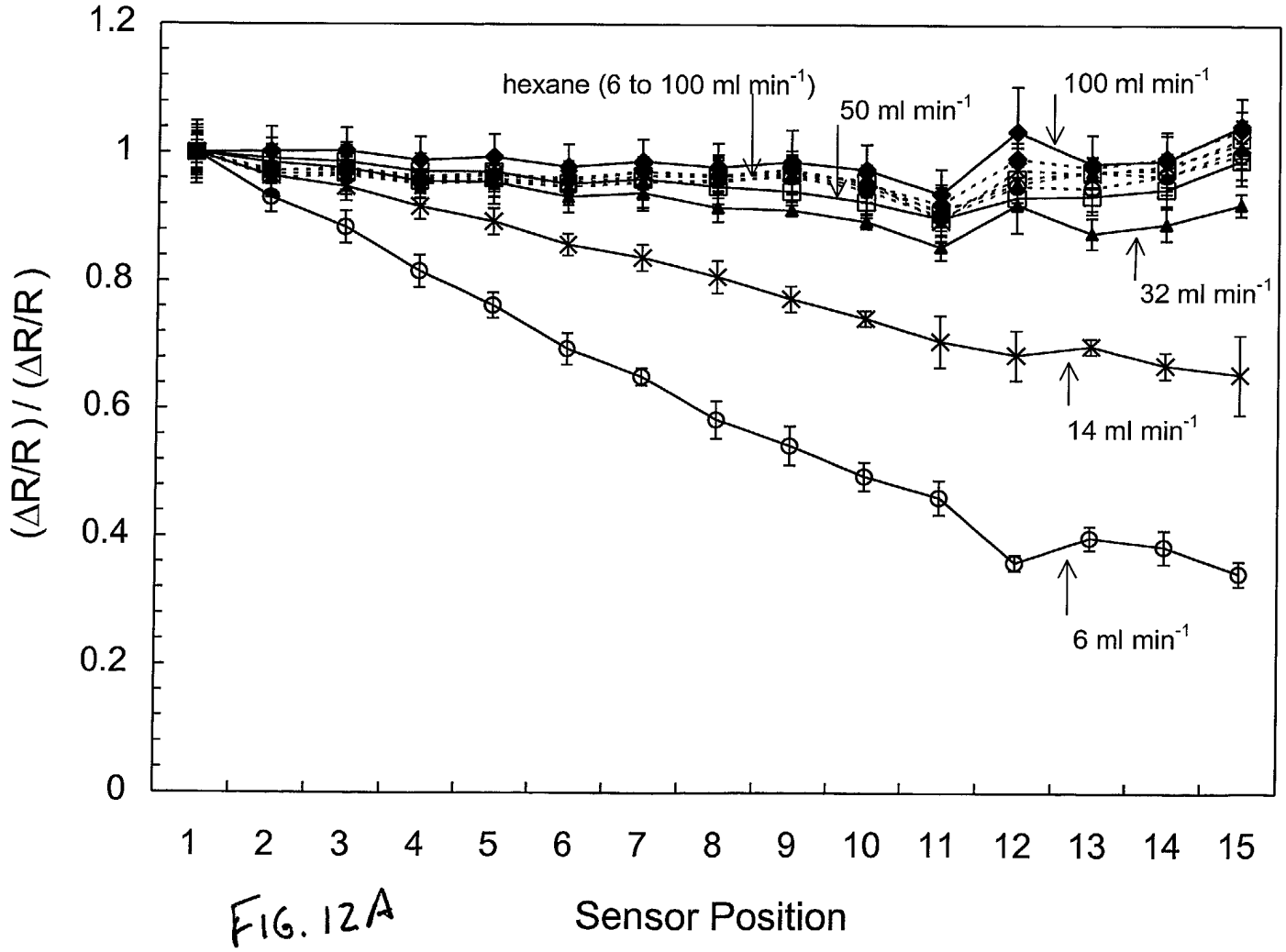
1.2
1
0.8
0.6
0.4
0.2
0
(ΔR/R) / (ΔR/R)
hexane (6 to 100 ml min-1)
50 ml min-1
100 ml min-1
32 ml min-1
14 ml min-1
6 ml min-1
1 2 3 4 5 6 7 8 9 10 11 12 13 14 15
Sensor Position

FIG. 12A

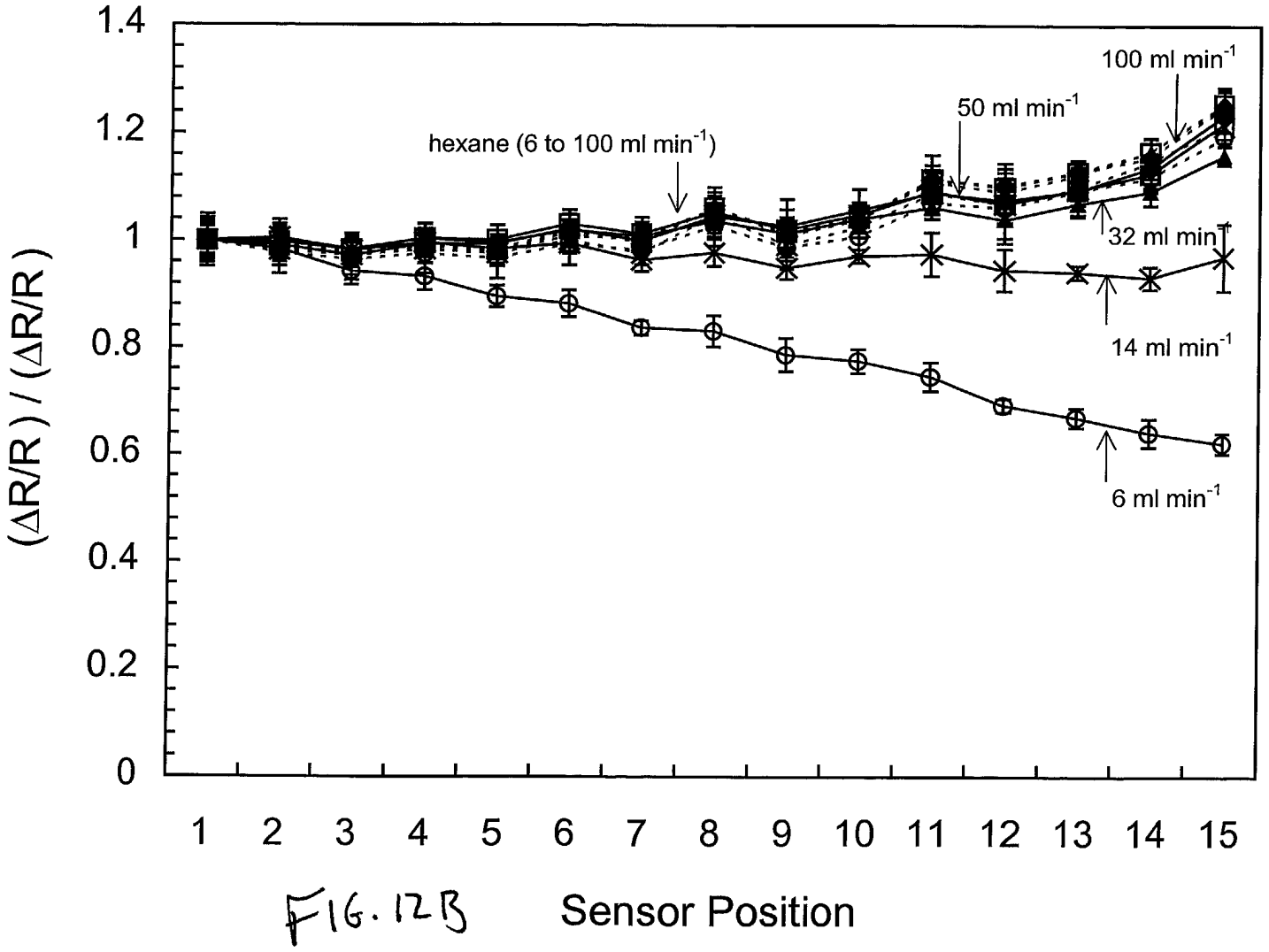
1.4
1.2
1
0.8
0.6
0.4
0.2
0
(ΔR/R) / (ΔR/R)
hexane (6 to 100 ml min-1)
100 ml min-1
50 ml min-1
32 ml min-1
14 ml min-1
6 ml min-1
1 2 3 4 5 6 7 8 9 10 11 12 13 14 15
Sensor Position

FIG. 12B

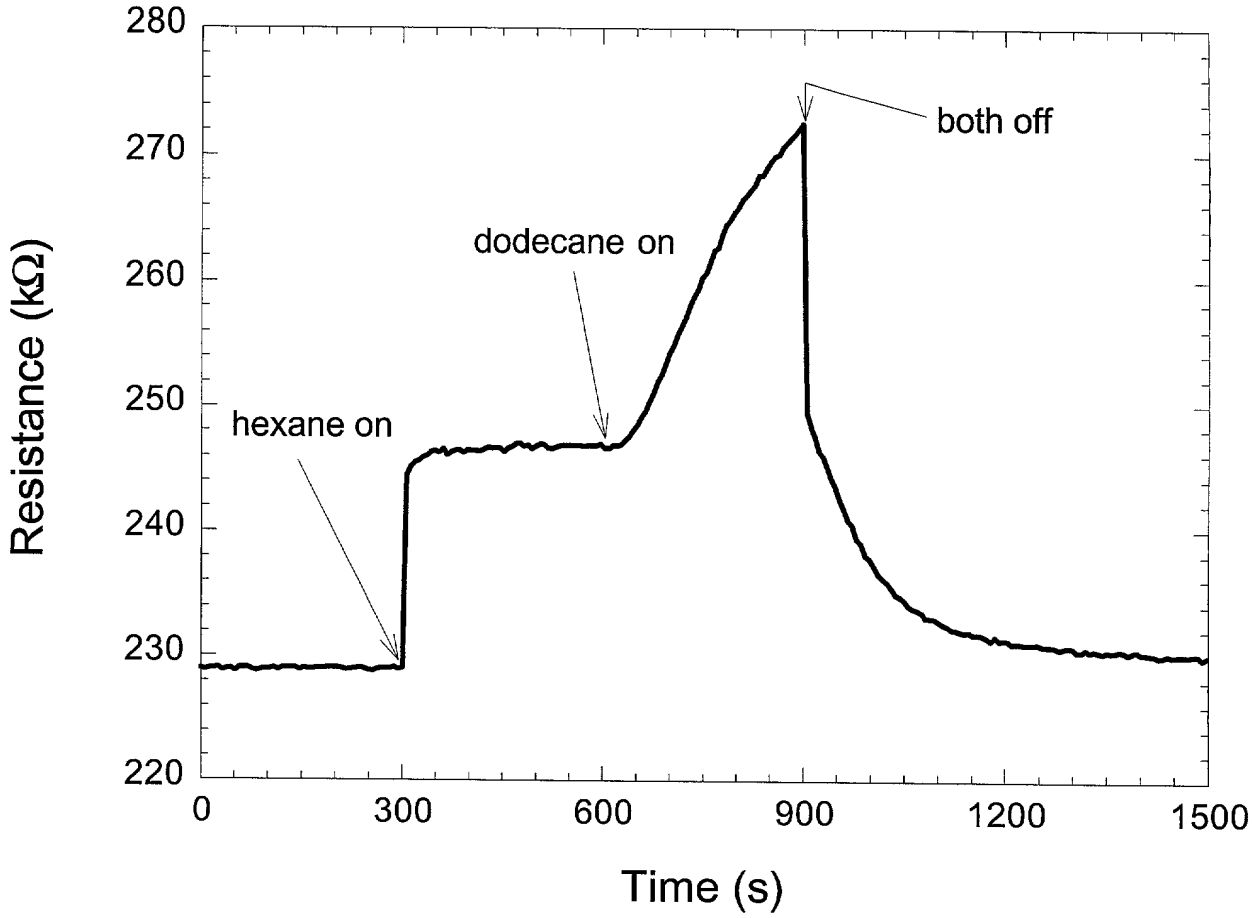
280
270
260
250
240
230
220
Resistance (kΩ)
0
300
600
900
1200
1500
Time (s)
hexane on
dodecane on
both off

FIG. 13

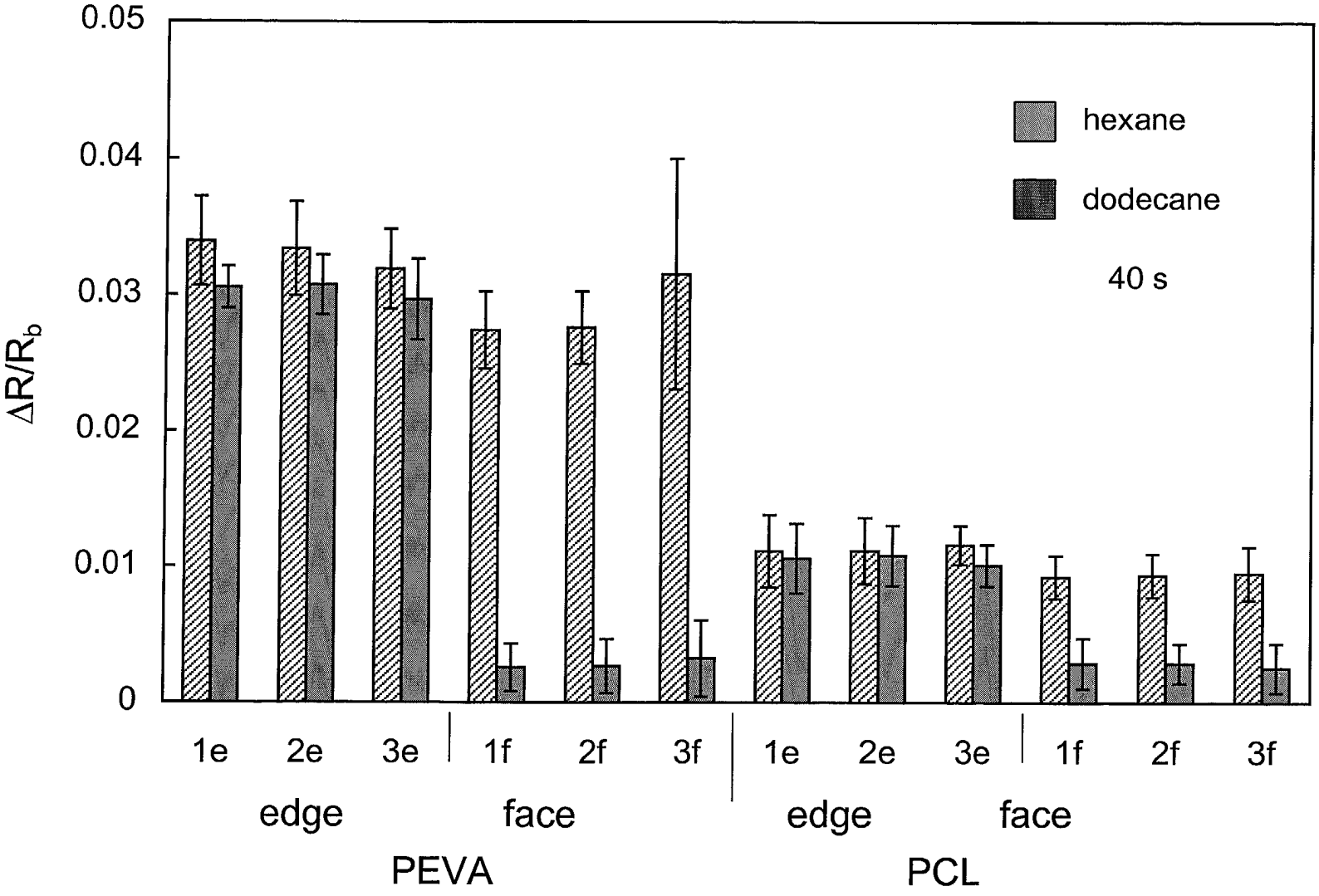
0.05
0.04
0.03
0.02
0.01
0
ΔR/R_b
hexane
dodecane
40 s
1e
2e
3e
1f
2f
3f
1e
2e
3e
1f
2f
3f
edge
face
edge
face
PEVA
PCL

FIG. 14A

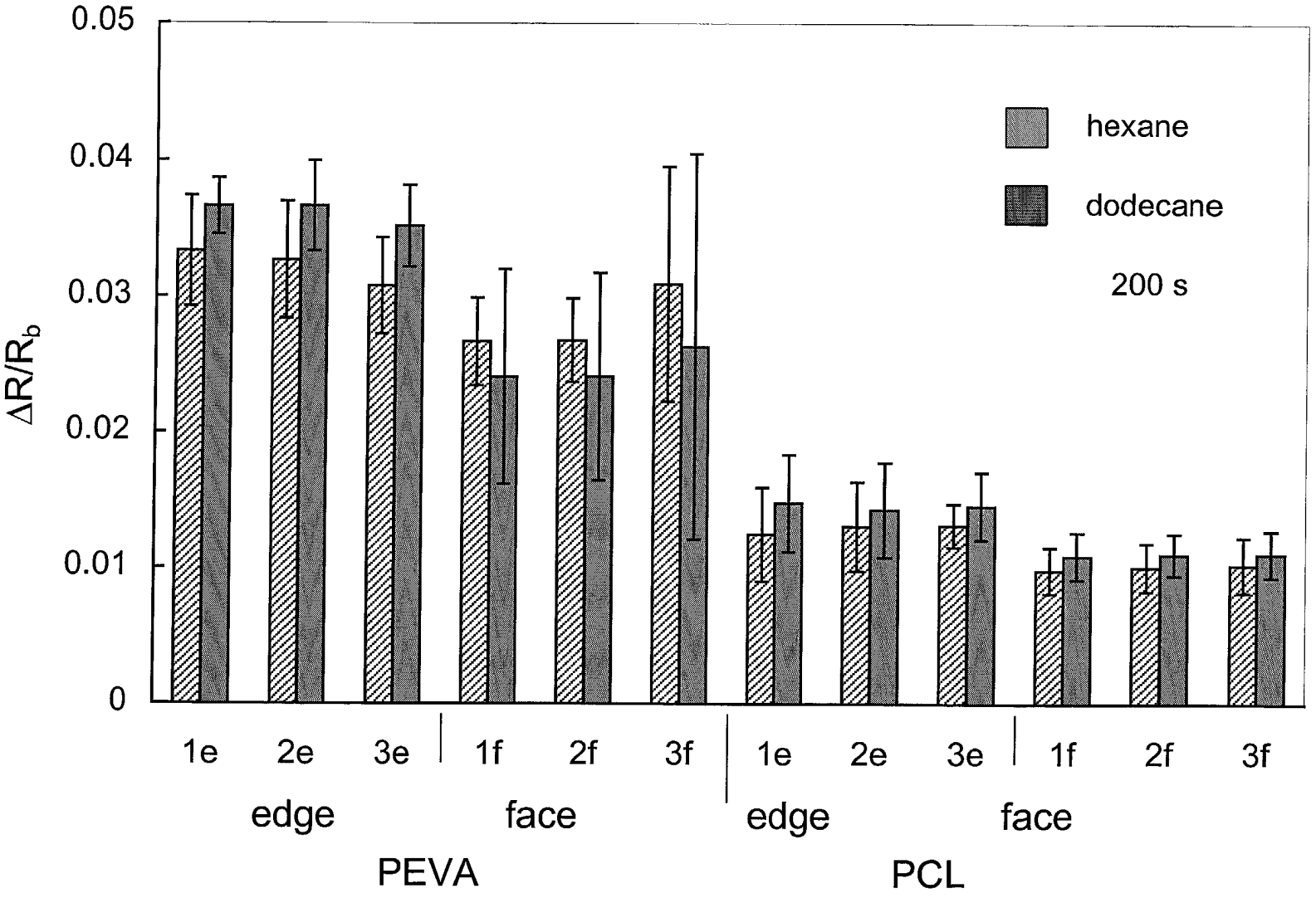
0.05
0.04
0.03
0.02
0.01
0
ΔR/R_b
hexane
dodecane
200 s
1e
2e
3e
1f
2f
3f
1e
2e
3e
1f
2f
3f
edge
face
edge
face
PEVA
PCL

FIG. 14B

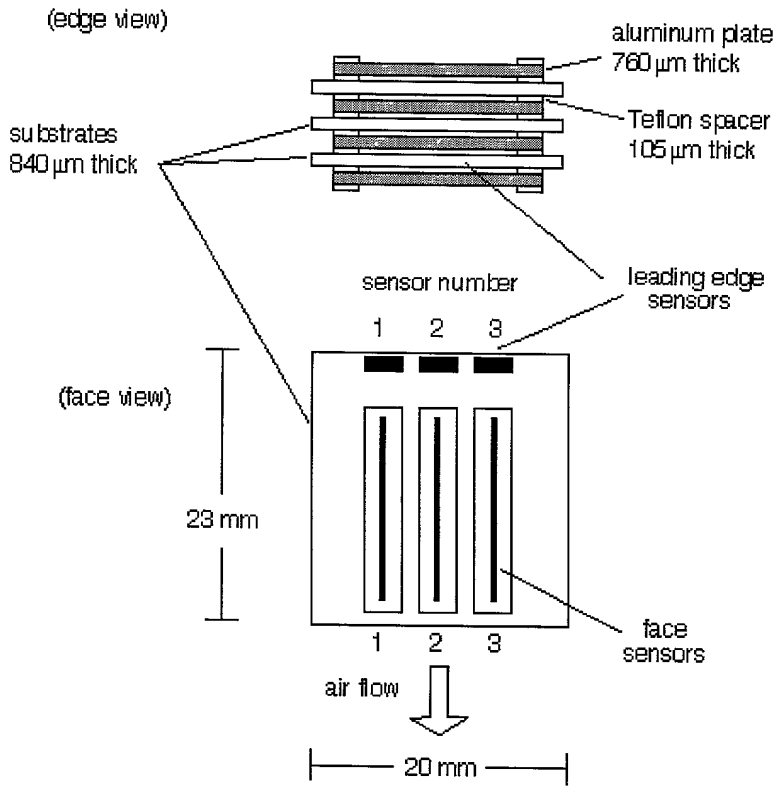
(edge view)
aluminum plate
760 µm thick
Teflon spacer
105 µm thick
substrates
840 µm thick
sensor number
leading edge
sensors
1 2 3
(face view)
23 mm
face
sensors
1 2 3
air flow
20 mm

FIG. 15

Raw Responses to Pure DNT Vapor Dilutions and DNT Vapor Dilutions Containing High Concentrations of Contaminant Vapors

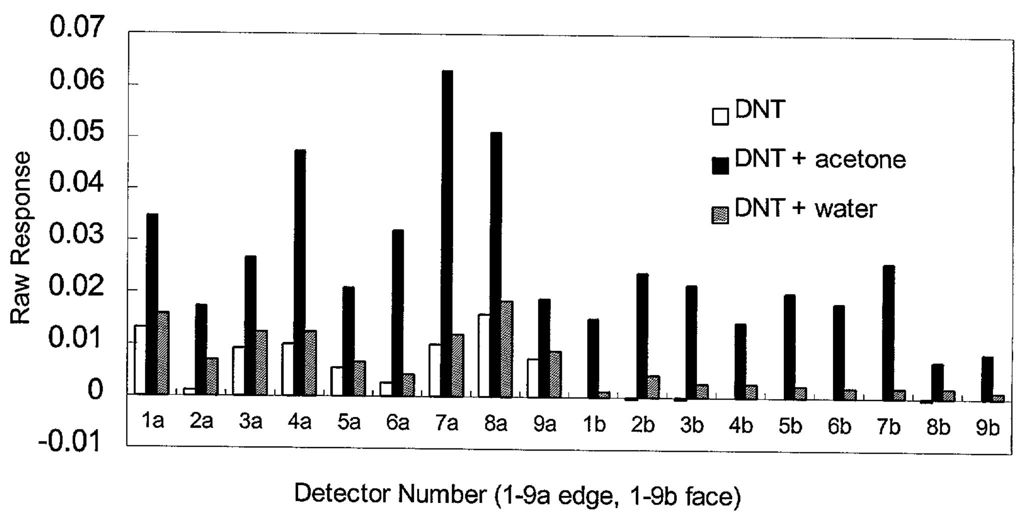

FIG. 16

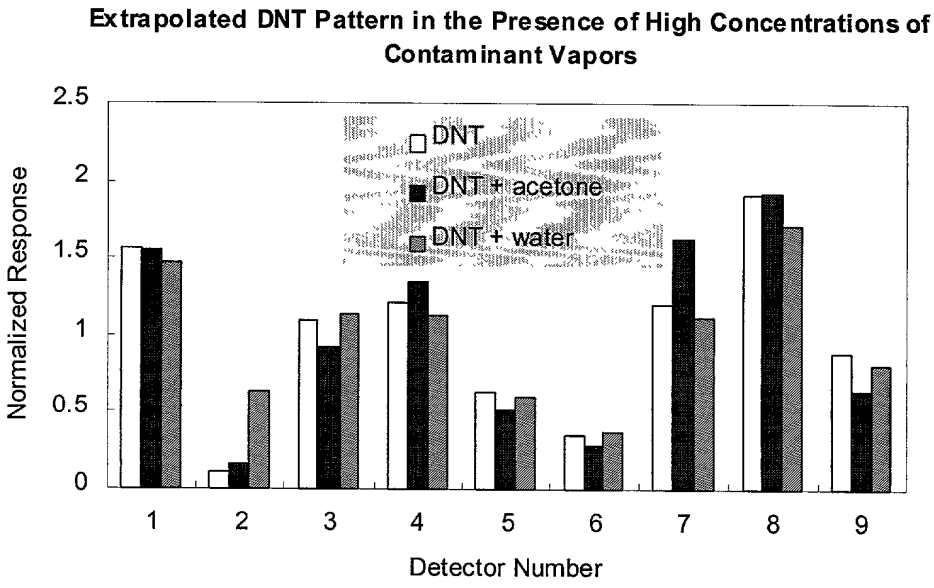
Extrapolated DNT Pattern in the Presence of High Concentrations of Contaminant Vapors
Normalized Response
2.5
2
1.5
1
0.5
0
DNT
DNT + acetone
DNT + water
1
2
3
4
5
6
7
8
9
Detector Number

FIG. 17